Towards axial capacity predictions through MWD data
what can we learn from installation efforts of drilled displacement piles

Figueroa, Genesis; Duffy, Kevin; NeSmith, Morgan; Lemnitzer, Anne

DOI
10.37308/DFIEFFC251550208

Publication date
2025

Document Version
Final published version

Citation (APA)
Figueroa, G., Duffy, K., NeSmith, M., & Lemnitzer, A. (2025). *Towards axial capacity predictions through MWD data: what can we learn from installation efforts of drilled displacement piles*. 94-103. Paper presented at DFI-EFFC International Conference on Deep Foundations and Ground Improvement, Bruges, Belgium. https://doi.org/10.37308/DFIEFFC251550208

TOWARDS AXIAL CAPACITY PREDICTIONS THROUGH MWD DATA: WHAT CAN WE LEARN FROM INSTALLATION EFFORTS OF DRILLED DISPLACEMENT PILES

Genesis Figueroa. Graduate Student Researcher, Univ. of California Irvine, Irvine, CA, USA
Kevin Duffy. Post-doctoral Researcher, Delft University of Technology, South Holland, The Netherlands
Morgan NeSmith. Director of Engineering, Berkel & Company Contractors, Inc., Atlanta, GA, USA
Anne Lemnitzer. Associate Professor, Univ. of California Irvine, Irvine, CA, USA, Corresponding author: alemnitz@uci.edu

ABSTRACT

The future of performance-based foundation design involves integrating Measurement-while-Drilling (MWD) data to enhance the resilience and construction efficiency of pile foundations. During the installation of Drilled Displacement Piles (DDPs), measurements include penetration speed (v_z), rotational speed (v_r), downward thrust, torque (T) or hydraulic pressure (P_{drill}). With these measurements in mind, data from 32 DDPs across 10 project sites in the US and Europe were collected and analyzed. A generalized formulation for installation effort was developed to compare existing pile databases with the data gathered by the authors. The proposed method uses a decomposed installation effort model that separately accounts for the shaft and toe portions of the pile. A regression analysis of the dataset shows the potential of using installation effort to predict pile capacity and provides fundamental knowledge towards establishing a basic framework for estimating pile load capacities during DDP installation. This application highlights the value of real-time monitoring data in performance-based foundation design.

Keywords: drilled displacement piles, measurement while drilling, axial capacity, screw displacement piles.

INTRODUCTION

During pile installation, data acquisition systems provide a significant amount of real-time information, commonly known as measurement-while-drilling (MWD) data. Building on the capability of this data is a rapidly growing research area in the industry (NeSmith and NeSmith, 2008). For drilled displacement piles (DDPs, also known as screw displacement piles in Europe), MWD data can be leveraged to (i) assess soil variability at the site (ii) quantify soil improvement, (iii) develop axial capacity predictions and (iv) optimize pile construction by balancing installation efficiency with satisfactory operational performance.

The drilling tool of a DDP consists of several auger flights near the tip, followed by an enlarged displacement body further along the pile length. Several different DDP designs and installation procedures are available in the industry, however, regardless of the type of drilling tool, each design aims for a combination of soil removal around the pile tip and soil displacement around the enlarged body, maximizing both installation efficiency and the pile's ultimate capacity. Key measurements during this process include penetration speed, rotational speed, crowd force on the pile head, and torque. Upon tool extraction, concrete volume and grout pressure are recorded, if applicable.

Installation procedures can have a significant effect on the pile capacity, as shown in both drilled displacement piles (van Impe, 2001; Siegel et al., 2007; Hird and Guymer, 2011; Pucker and Grabe, 2012) and in screw anchors and auger piles (Brown, 2005; Cerfontaine, 2023). For instance, the theoretical framework and model tests by Slatter (2000) show how the radial stresses acting on a DDP depend on the combined process of soil transport, soil displacement, and the installation torque during pile installation. However, no industry-wide consensus has been established on how DDP installation and tool geometry impact the pile's ultimate capacity, largely due to the lack of publicly available, full-scale, pile load tests where the pile base and shaft resistances have been directly measured.

Towards the goal of exploring the effect of drilling parameters on the capacity of full-scale DDP piles, this paper presents the first step of the authors' research by revisiting and building upon existing correlations between the installation effort and pile capacity, showing how MWD data could be used to quantify installation efforts with more certainty and how to make them a useful tool to aid in the design of drilled displacement piles in the future.

DDP DATABASE AND ANALYSIS

Data analyzed in this paper was generously provided by members of the Deep Foundation Institute's ACIP and DD technical committee and the archives of TU Delft in the Netherlands. In these projects De Waal, Auger Pressure Grouted Displacement (APGD), and Omega piles were constructed, and drilling data was recorded. Static axial load tests following the American (ASTM D1143) and Dutch (NPR 7201) codes were performed to determine the axial capacity of the DDPs. The authors reviewed all project data to ensure uniform site information and consistent data quality across all projects, including: the type of displacement tool, in-situ soil testing, the availability of groundwater table locations, and the availability of key MWD data such as the penetration speed (v_z) and the hydraulic pressure (P_{drill}). When pile load testing on the site exhibited a clear, in-situ, plunging behavior, the ultimate bearing capacity of the piles (Q_{u}) was calculated using the Modified Davisson Offset Limit method adjusted for other pile types following Perlow's (2020) recommendations. Van der Veen's (1953) method was applied to extrapolate test data when no failure was observed experimentally. The axial load at a pile head settlement equal to 10%D ($Q_{10\%\mathrm{D}}$) was also recorded when available (Table 1). DDPs in the database were installed in different soil profiles such as homogeneous cohesionless soils, homogeneous cohesive soils, and stratified soil profiles. Therefore, both, friction piles as well as end-bearing piles, were represented.

Data analysis

NeSmith and NeSmith (2008) introduced an "Installation Effort" (Eq. 1) and compared it to the pile's total capacity (Q_u) observed in the field. This database was entirely developed for Berkel's APGD piles. The authors considered two key drilling parameters: the Torque Index (*TI*) calculated from the hydraulic drilling pressure, and the Penetration Rate Index (*PRI*) calculated from the penetration speed (v_z) of the drilling tool. The coefficients in Eq. 1 were defined based on the company-specific drill rig. The base penetration rate (PR_{base}) is the rate at which the gearbox moves vertically with no resistance and was defined as 0.1 m/s (20 ft/min). The base torque (T_{base}) is the required torque to turn the gearbox with no soil resistance at maximum rotation rate. This parameter was defined as 10 MPa (100 bars). The cumulative installation effort ($\mathrm{IE}_{\mathrm{cum}}$ - Eq. 2) was calculated by summing the IE for every 30 cm (1 ft) along the pile.

To compare the new database collected by the authors to the original NeSmith & NeSmith (2008) database, the installation effort proposed by NeSmith & NeSmith (2008) was modified to remove the rig-specific fitting coefficients PR_{base}, and T_{base}. A new Cumulative Installation Effort was defined as IE_{2cum}. Eqs. 3-5 explain the derivation of this modified installation effort, where *PR* (or v_z) and T (or P_{drill}) are in ft/min and bar, respectively. In Eq. 3 the terms $\mathrm{PR}_{\mathrm{base}}$ and $\mathrm{T}_{\mathrm{base}}$ were removed from the summation as they are common factors at each depth. By solving for PR_{base}, and T_{base} equal to 0.1 m/s (20 ft/min) and 10MPa (100bars), respectively, Eq. 4 is obtained. Eq. 5 shows the new $\mathrm{IE}_{2\mathrm{cum}}$ and its relationship with NeSmith and NeSmith (2008) IE.

Table 1. Overall information of each project site and tested piles

Project Site	Pile	GWT Depth [m]	Tool	D [cm]	L [m]	Grout Factor	Average vz [m/s]	Average Pdrill [MPa]	Qu [kN]		$Qu_{10\%D}$ [kN]
PS1	P1	1.2	Omega	40.6	20.3	1.2	0.06	16.9	2139	*	-
	P2	**1.2**	**Omega**	**40.6**	**19.8**	**1.2**	**0.07**	**17.6**	**1601**	*	**-**
	P3	**1.2**	**Omega**	**40.6**	**19.6**	**1.1**	**0.13**	**15.8**	**1334**	*	**1334**
	P4	1.2	Omega	40.6	19.6	1.1	0.08	17.0	1512	*	-
PS2	P5	5.2	APGD	40.6	22.9	1.3	0.03	21.5	5649		-
	P6	5.2	APGD	40.6	21.3	1.3	0.04	18.3	5084		-
	P7	5.2	APGD	40.6	19.8	1.3	0.03	15.8	5178		-
PS3	**P8**	**3.0**	**DeWaal**	**35.6**	**16.5**	**1.2**	**0.04**	**12.7**	**2945**		**1196**
	P9	3.0	DeWaal	35.6	15.2	1.2	0.04	12.8	3114		1744
	P10	3.0	DeWaal	35.6	14.9	1.2	0.05	11.9	2242	*	-
	P11	3.0	DeWaal	35.6	13.1	1.2	0.05	11.2	1794	*	2242
	P12	3.0	DeWaal	35.6	11.6	1.2	0.05	10.5	1146	*	-
PS4	P13	1.2	DeWaal	45.7	9.1	1.2	0.05	16.4	1001	*	1036
	P14	1.2	DeWaal	45.7	16.8	1.2	0.04	17.2	1753	*	1893
	P15	1.2	DeWaal	61.0	9.1	1.2	0.05	18.6	1570	*	1475
PS5	P16	2.4	DeWaal	40.6	8.5	1.2	0.04	21.0	1794	*	1789
	P17	2.4	DeWaal	40.6	10.1	1.3	0.06	20.7	1873	*	1875
PS6	P18	3.7	DeWaal	45.7	15.2	1.3	0.10	14.4	1654	*	1794
	P19	3.7	DeWaal	45.7	15.2	1.3	0.08	13.8	1694	*	1702
PS7	P20	6.1	DeWaal	35.6	9.1	1.2	0.04	6.4	3089	*	2740
	P21	6.1	DeWaal	35.6	7.9	1.2	0.05	3.3	2431	*	2204
PS8	P22	0.5	DeWaal	40.6	23.8	1.2	0.06	16.6	2765		-
	P23	0.5	DeWaal	40.6	21.6	1.2	0.06	16.5	2541	*	2508
	P24	0.5	DeWaal	35.6	24.4	1.3	0.06	17.5	3090		-
	P25	0.5	DeWaal	35.6	22.3	1.3	0.05	17.3	2989		-
PS9	P26	1.5	DeWaal	40.6	17.4	-	0.13	13.6	2402	*	2370
	P27	1.5	DeWaal	40.6	17.9	-	0.13	14.1	2406	*	-
	P28	1.5	DeWaal	40.6	17.4	-	0.12	13.8	2306	*	2306
	P29	1.5	DeWaal	40.6	17.9	-	0.11	14.8	2157	*	2158
PS10	P30	1.5	DeWaal	35.6	16.0	-	0.09	13.8	1487	*	1485
	P31	1.5	DeWaal	35.6	16.5	-	0.11	13.2	1157	*	1092
	P32	1.5	DeWaal	35.6	16.5	-	0.10	13.9	996	*	945

*: Pile reached an in-situ axial load failure

$$IE = PR_{index} * T_{index} = \left[\frac{1}{\sqrt{PR/PR_{base}}}\right] * \left[2.7815 * \left(\frac{T}{T_{base}}\right)^{1.3629}\right] \quad [1]$$

$$IE_{cum} = 2.7815 * \sum \frac{1}{\sqrt{PR/PR_{base}}} * \left(\frac{T}{T_{base}}\right)^{1.3629} \quad [2]$$

$$IE_{cum} = 2.7815 * \frac{\sqrt{PR_{base}}}{T_{base}^{1.3629}} * \sum_{z=0}^{z=L} \frac{T_z^{1.3629}}{\sqrt{PR_z}} \quad [3]$$

$$IE_{cum} = 0.00234 * \sum_{z=0}^{z=L} \frac{T_z^{1.3629}}{\sqrt{PR_z}} \quad [4]$$

$$\frac{IE_{cum}}{0.00234} = \sum_{z=0}^{z=L} \frac{T_z^{1.3629}}{\sqrt{PR_z}} = IE_{2.cum} \quad [5]$$

Figure 1 presents the results of the IE_{2cum} calculations. Fig. 1(a) plots the cumulative IE_{2cum} vs. the piles' ultimate capacity Q_u, and Fig. 1(b) presented the cumulative IE_{2cum} vs. the pile capacity at a displacement corresponding to 10% of the pile diameter ($Q_{10\%D}$). Both graphs suggest that high variability exists for a given installation effort. For example, as shown in Fig. 1a, an $IE_{2,cum}$ of 30,000 corresponds to a pile capacity ranging from 1500 to 4000 kN. The high variability in measured pile capacity may suggest that local geology or minerology, pile tip resistance, ground water conditions and tool geometry can have an influence on the installation-capacity correlation (NeSmith and NeSmith, 2008). It also cautions a general application of a method that simply sums MWD data without the consideration of local geology.

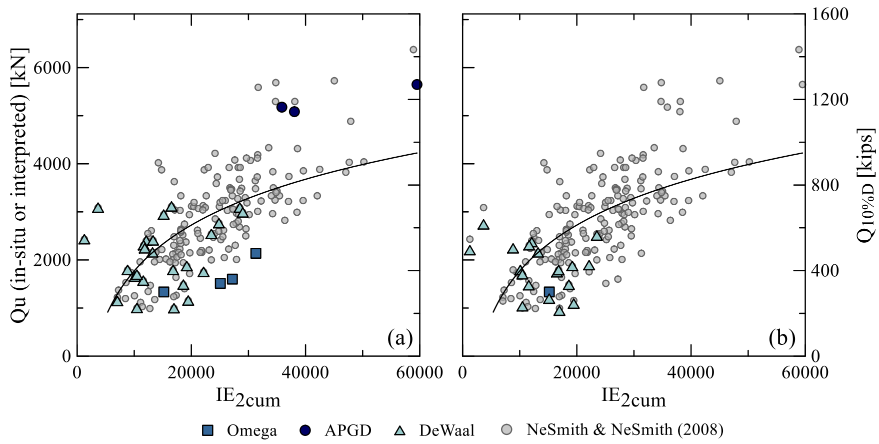

Fig. 1. IE_{2cum} vs. (a) Ultimate axial load (Qu), (b) at a settlement equal to 10%D ($Q_{10\%D}$).

Analysis of three pile installations

To illustrate the impact of site-specific factors on the installation effort, three representative sites were selected from the database, as shown in Fig. 2-4. These sites were chosen to assess piles with different IE_{2cum} reaching a similar axial failure load (P2 and P3), and piles with a similar IE_{2cum} but different axial load behavior (P3 and P8). Cone penetration tip resistance (q_t in Fig. 2-4) suggests that all piles (P2, P3 and P8) are installed in similar, primarily clayey soils sites. The soil behavior type index I_c (Robertson 2014) ranges between 2.5-3.5.

Piles P2 and P3 have nearly identical pile geometries (D, L) and were installed at the same project site using the same displacement tool. Pile P2 was installed with a consistent downward speed v_z of 10 cm/sec until a stronger layer was encountered (~10 m depth). Consequently, the installation speed decreased, and the drilling pressure increased. Thereafter, the drilling tool continued with the same initial linear downward trend observed in the upper layer (Fig. 2c).

Pile P3 was advanced at a much faster rate, reaching a penetration speed 1.5 times higher than pile P2 (Fig. 3d). The same installation trends can be observed as P3 enters the strong layer at 10m depth, however slightly less drilling pressure was applied due to the initially higher downward speed. (i.e., faster advancement through the stronger layer). P3 therefore has a lower IE_{2cum} due to the inverse relationship of v_z in the IE_{2cum} equation.

Pile P8 was installed with a much slower downward advancement of only 5cm/sec (or less) and tipped in a stronger bearing layer starting around 12m of depth. A reduction in penetration speed (v_z) and increase in drilling pressure (P_{drill}), is evident when entering the strong bottom layer of site P8 (see Fig. 4(a) and (c)).

Figure 5a-c shows the individual IE_2 with depth during the installation of P2, P3, and P8. The individual IE is the installation effort required to penetrate one foot of soil, and is represented by one data point every foot. Figure 5d shows the cumulative (total) Installation Effort2 (IE_{2cum}-Fig. 5d) of all three piles. This value represents the sum of the installation effort up to the respective pile length/depth. Hence, the last data point represents the effort to install the entire pile length. Fig. 5 also shows the soil behavior type defined based on the I_c (Robertson 2014).

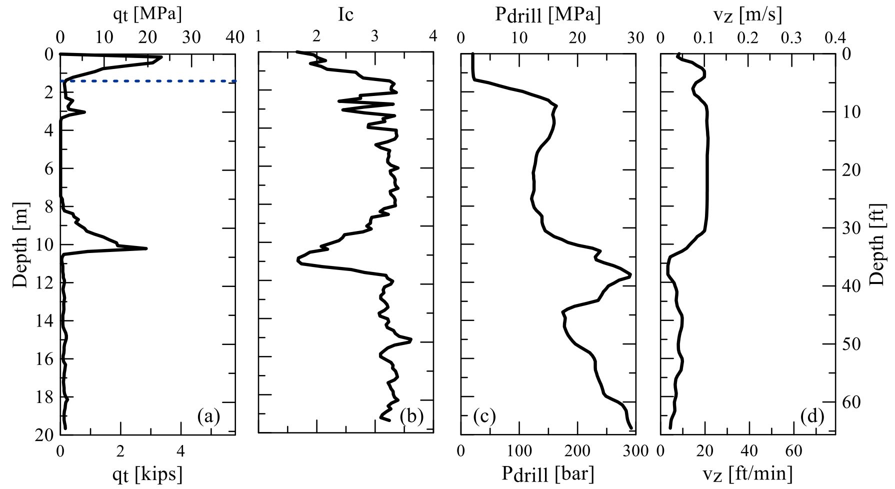

Fig. 2. P2 data: (a) q_t, (b) I_c, (c) P_{drill}, (d) v_z.

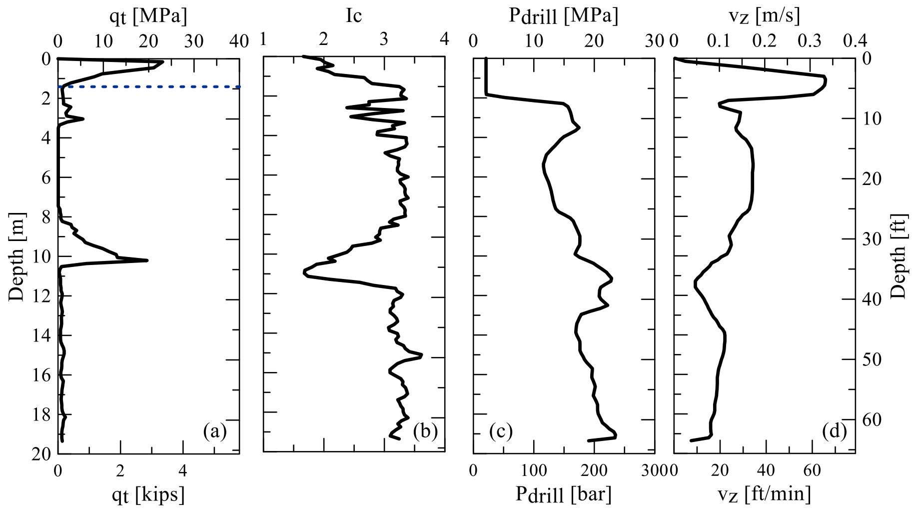

Fig. 3. P3 data: (a) q_t, (b) I_c, (c) P_{drill}, (d) v_z.

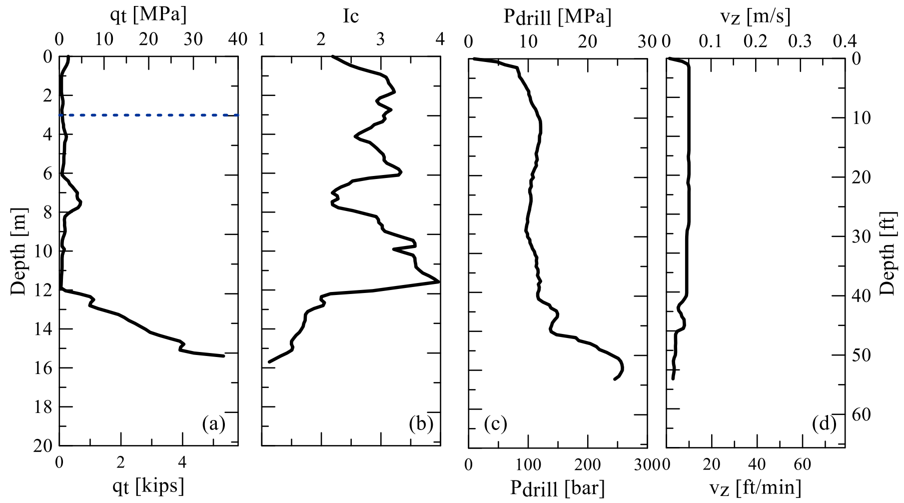

Fig. 4. P8 data: (a) q_t, (b) I_c, (c) P_{drill}, (d) v_z.

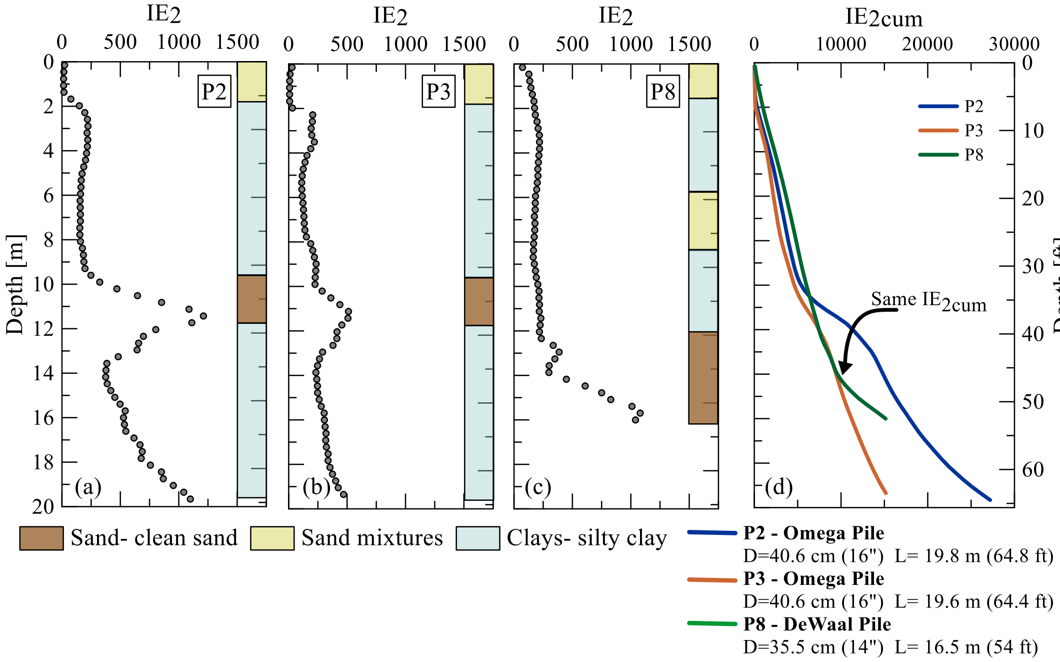

Fig. 5. IE_2 at all depths for (a) P2, (b) P3, and (c) P8. IE_{2cum} for all three piles.

Piles P2 and P3 have an intermediate clean sand layer from 9.5 to ~11.5m with a q_t ranging from 5 to 20 MPa; a significant increase in the IE_2 can be observed at this depth for both piles as the tool pushes through the stronger layer (Fig. 5). Pile P8 also has a sandy layer from 6 to 8 m, however this layer has an average q_t of less than 5MPa, and consequently, not much variation of the IE_2 is observed at this depth. A significant increase of the IE_2 can be observed when P8 reached the clean sand layer at 12m (target bottom layer for pile tip).

Figure 5d shows that piles P2 and P3 follow a very similar cumulative installation effort IE_2. For instance, at a depth of 14m the cumulative IE_2 is the same for P3 and P8 regardless of which layers are along the pile shaft; i.e., the cumulative installation effort does not recognize whether the pile passes through an intermediate (strong) bearing layer or whether this layer is reached at the end (e.g. for Pile 8). Pile P8 only begins to show a significant increase in installation effort after reaching the bottom clay layer.

In contrast, when comparing P2 and P8 (Fig. 5d), both piles show a similar installation effort until about 10m of depth, followed by a divergence of IE due to the speed and pressure applied to P2 while passing the stronger sand layer. At about >16m depth, both piles approach similar installation efforts.

These discrepancies can lead to a wrong interpretation of the axial load capacity for both P3 and P8 (Fig. 6).

Although IE_{2cum} for P2 (~28000) is almost twice the IE_{2cum} for P3 (~15000), the axial load tests on both piles show similar capacities. On the other hand, when comparing P3 and P8, both piles were installed at different sites under different installation conditions and geometries. Both piles have similar IE_{2cum} but significantly different failure capacities. P8 has more than twice the capacity of P3. Given the soil conditions at both sites, it's likely that both piles mobilized their base and shaft capacities very differently—with P3 predominantly a shaft-bearing pile and P8 predominantly an end-bearing pile. Hence it is important to understand the mechanisms which contribute to developing the total axial pile capacity (friction or end-bearing). When the cumulative installation effort is calculated, the location of a strong layer does not play a significant role since all the effort is lumped into a single value (IE_{2cum}).

Decomposition of installation effort

While the concept of cumulative installation efforts captures the overall pile installation effort, recognizing individual contributors, such as end-bearing, shaft friction, or overburden stresses is critical. Separation of parameters is also important for developing future correlations between the IE and axial design capacities; especially since most design approaches rely on increased resistance with increasing depths. To demonstrate this further, the installation effort was decomposed into friction and end-bearing components.

To reiterate, the piles' individuals IE_2s were calculated at foot-long increments (Fig. 5a-c – Eq. 5) and the cumulative value (IE_{2cum}) was calculated by summing the IE_2 along the pile depth until the desired pile embedment is reached (Fig. 5d). The cumulative effort IE_{2cum} was divided into pile shaft and pile toe . The effort attributed to the pile toe was taken as the sum of IE_2 in a zone 4D above the pile toe.

Figure 7 shows the $IE_{2.shaft.cum}$, $IE_{2.toe.cum}$, and the IE_{2cum} for piles P2, P3, and P8. It is evident that piles P2 and P8 require a substantial installation effort in the region of the pile toe, which agrees with the individual installation effort variation shown in Fig. 5. This observation is likely associated with the effects of overburden pressure and soil densification at lower depths and does not necessarily imply that the pile is an end-bearing pile (see example of P2). Figure 7 shows the percentage contribution of the $IE_{2.shaft.cum}$, $IE_{2.toe.cum}$ in the total cumulative IE_{2cum}. It can be observed that for P8 (end-bearing pile) the cumulative installation effort in the toe area represents a quarter of the total effort when constructing the pile.

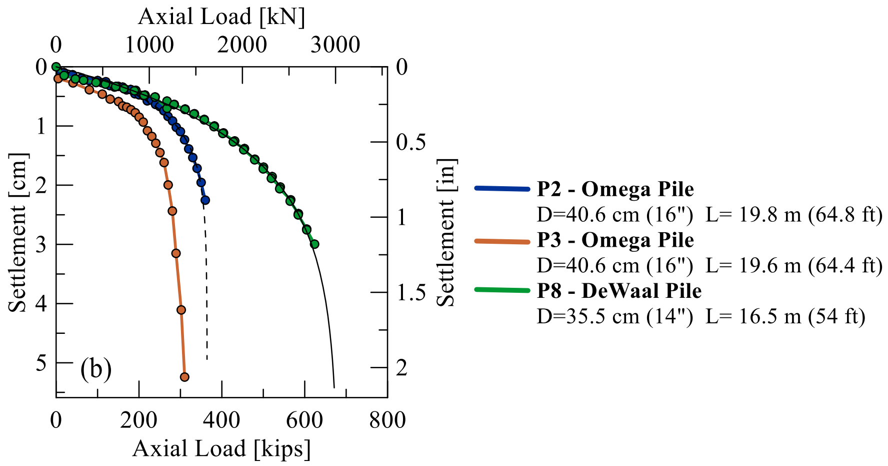

Fig. 6. Comparison between P1, P3, and P12 (a) IE_{2cum}, and (b) axial load test results.

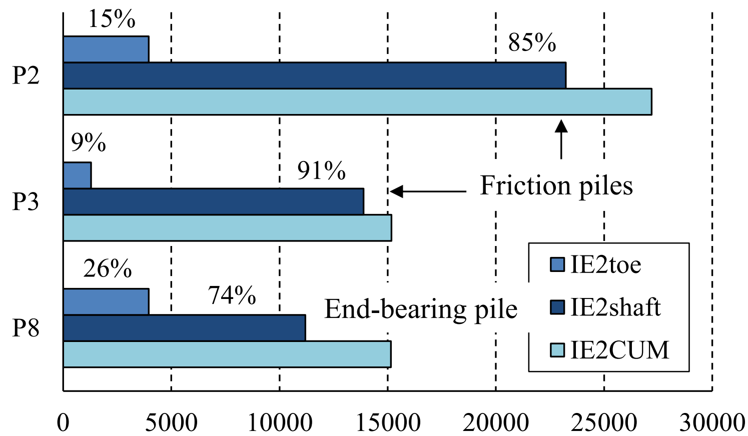

Fig. 7. $IE_{2.shaft}$, $IE_{2.toe}$, and IE_{2cum} for piles P2, P3, and P8.

The average IE_2 in the shaft ($IE_{2.\text{shaft.ave}}$) and toe area (4D above pile toe - $IE_{2.\text{toe.ave}}$) was obtained to compare the overall effort in both zones. A simple linear regression analysis of $IE_{2.\text{shaft.ave}}$, $IE_{2.\text{toe.ave}}$, and $IE_{2\text{cum}}$ was carried out to understand the importance of each IE_2 component when predicting the axial load capacity of the piles. This purely mathematical analysis led to the derivation of Equation 6. Equation 6 presents a prediction of ultimate pile capacity and the components of the installation effort in terms of shaft friction and toe resistance. This equation was only derived for P2, P3, and P8, and is intended to emphasize the importance of the distinction between the shaft and toe IE_2. The weighted factors preceding each component shown in Eq. 6 demonstrate the significance of the installation effort while drilling in the toe area, ≈4 times the IE_2 at the pile's shaft. To reiterate this does not mean that the pile is necessarily an end-bearing pile, the weighted factor simply accounts for the stronger (and likely more compressed) soil layers at greater depths. It indirectly accounts for the effects of overburden pressure on the soil-pile resistance and follows the same linear trend as shown by the general increase of drilling pressure (P_{drill}) with depth (Figs 2-4). Table 2 compares the predicted capacity ($Q_{u.MWD}$) calculated with Eq.6 with the measured capacities in the field. Pile capacities calculated from the installation efforts yielded predictions within 5% accuracy of the measured failure load on site.

$$Q_{u.MWD}[kN] = \frac{10000*(4.46IE_{2.\text{toe.ave}}+1.13IE_{2.\text{shaft.ave}})}{IE_{2.\text{cum}}} \quad [6]$$

Table 2. Predicted ultimate load ($Q_{u.MWD}$) with $IE_{2.\text{shaft}}$, $IE_{2.\text{toe}}$, and the $IE_{2\text{cum}}$.

Pile	$Q_{u.test}$ [kN]	$IE_{2\text{shaft.ave}}$	$IE_{2\text{toe.ave}}$	$IE_{2\text{cum}}$	$Q_{u.MWD}$ [kN]
P2	1627	370	931	27194	1682
P3	1356	222	392	15178	1320
P8	2992	221	955	15156	2977

The close agreement between predictions and in-situ measurements is expected, given the limited number of case histories in the regression model, but it highlights the potential of this analytical approach. It also demonstrates the use of decomposed installation efforts to predict the axial load capacity of drilled displacement piles.

SUMMARY AND CONCLUSION

The future of performance-based foundation design integrates MWD data to improve pile foundation resilience and efficiency. During Drilled Displacement Pile (DDP) installation, key parameters such as penetration speed, rotational speed, thrust, torque, and hydraulic pressure are measured. Data from 32 DDPs across 10 sites in the US and Europe were analyzed. The analysis of a cumulative installation effort revealed that in order to establish a reliable method for using installation effort as correlation between axial pile capacity and MWD parameters, a simplified 2D analysis ($IE_{2\text{cum}}$ vs. axial capacity) is insufficient. While the cumulative installation effort effectively represents the total energy exerted during pile installation by summing parameters up to a given depth, it is essential to consider its individual contributions.

A regression analysis performed on the three case histories presented in this paper demonstrates how the separation of installation effort in shaft and toe installation efforts changes the predictive accuracy. A prototype equation to estimate axial pile capacities, currently only applicable to the small dataset presented herein, demonstrates the potential of more accurately estimating the axial pile capacity compared to previously developed correlations. Using the equation proposed herein, a predicted pile capacity within 5% of the measured capacity in the field was obtained.

The authors aim to refine and expand this model by incorporating key geotechnical parameters (e.g., σ_z, or GWT) and additional soil characterization indices. Geological variability, soil angularity, and site-specific factors also affect the improvement achieved by the displacement tool, influencing axial load and settlement performance. Operator skill and rig-specific features further contribute to variability, particularly in drilling pressure and tool geometry. As such, the authors are actively expanding their pile database and refining this framework to develop a predictive design model, capable of integrating high-quality site data and MWD records for diverse soil conditions and DDP tools. Ongoing work includes data collection and analysis, as a larger database will help refine the general functional relationships between the DDP tool, geometry, MWD data, and pile behavior.

ACKNOWLEDGEMENTS

This research was primarily supported by the DFI Technical Committee fund. Partial support was also obtained from grant CMMI 1752303 sponsored by the National Science Foundation of the United States. We gratefully acknowledge the following professionals and companies for their support of this project and their willingness to share data generously: Sam Warren (Farrell Design-Build, Inc.), Piyush Sharma and Danny Cohen (formerly @ Morris-Shea Bridge Co., Inc.), Tim Siegel (Dan Brown & Associates), and Berkel & Company Contractors, Inc.

REFERENCES

ASTM (American Society for Testing and Materials) (2020). *Standard Test Methods for Deep Foundation Elements* Under *Static Axial Compressive Load*. ASTM International, Standard D1143M. West Conshohocken, PA. doi: 10.1520/D1143_D1143M-20.

Basu, P., Prezzi, M., Basu, D. (2010). Drilled displacement piles: Current practice and design. DFI Journal - *The Journal of the Deep Foundations Institute* 4(1):3–20. https://doi.org/10.1179/dfi.2010.001

Brown, D. A. (2004). Practical considerations in the selection and use of continuous flight auger and drilled displacement piles. *Advances in Designing and Testing Deep Foundations*, 251-261. https://doi.org/10.1061/40772(170)4

Cerfontaine et al. (2023). Control of screw pile installation to optimize performance for offshore energy applications. Géotechnique, 73(3), 234-249. https://doi.org/10.1680/jgeot.21.00118

Figueroa, G., Vrugt, J., Lemnitzer, A. (2024). Evaluation of soil improvement surrounding drilled displacement piles through pre- and post-installation CPT data. *Manuscript in review, Acta Geotechnica*

Hird, C.C., Ni, Q., Guymer, I.: Physical modeling of deformations around piling augers in clay. *Geotechnique* 61(11), 993–999 (2011)

NEN (Dutch Standardisation Insitutue) 2020. Geotechniek-Bepaling van het axiaal draagvermogen van funderingspalen door middel van proefbelastingen [Geotechnics–Determination of the axial capacity of foundations pile through load tests]. [In Dutch.] NPR 7201:2017 +A1. Delft, Netherlands: NEN.

NeSmith, W. M., & NeSmith, W. M. (2006). *Anatomy of a data acquisition system for drilled displacement piles*. GeoCongress 2006, 1-6. https://doi.org/10.1061/40803(187)67

NeSmith, W. M., & NeSmith, W. M. (2008). I*nstallation Effort: Current Calculation Methods and Uses in Design and Construction in the U.S*. 5th International Geotechnical Seminar on Deep Foundations on Bored and Augered Piles. Ghent, Belgium.

Perlow M. (2020). *A soil quake Davisson Offset Method for Drilled Foundations*. Deep Foundation Institute 45th Annual Conference, USA, Red Hook, NY, 183

Pucker, T., Grabe, J.: Numerical simulation of the installation process of full displacement piles. *Comput. Geotech*. 45, 93–106 (2012)

Robertson, P. K., Cabal K. L. (2014). Guide to Cone Penetration Testing for Geotechnical Engineering. Gregg Drilling & Testing, Inc., p 108-116.

Siegel, T. C., NeSmith W. M., NeSmith W. M., Cargill, P. E. (2007). *Ground Improvement resulting from Installation of Drilled Displacement Piles*. Proceedings, DFI's 32nd Annual Conference on Deep Foundations, Colorado Springs, CO, October 11-13, 2007.

Slatter, J. W. (2000). The fundamental behaviour of displacement screw piling augers. PhD Thesis, Monash University. pp 193.

Van der Veen, C. (1953). *The bearing capacity of a pile.* Proceedings of the 3rd International Conference on Soil Mechanics and Foundation Engineering, 2, 84-90.

Van Impe, W.F. (2001). Considerations on the influence of screw pile installation parameters on the overall pile behaviour. Proceedings of the Symposium on Screw Piles. Brussels, Belgium, 127-149.